JOURNAL OF MATERIALS SCIENCE 28 (1993) 659–668

Synthesis of ultra-fine SiC powders in a d.c. plasma reactor

C. W. ZHU, G. Y. ZHAO, V. REVANKAR, V. HLAVACEK*
Laboratory for Ceramic and Reaction Engineering, Department of Chemical Engineering, State University of New York at Buffalo, Buffalo, NY 14260, USA

Synthesis of SiC powder in a 15 kW d.c. plasma reactor by using the reaction systems of $SiCl_4 + CH_4$ and $CH_3SiCl_3 + CH_4$ was studied. The powder produced was characterized by X-ray diffraction and electron microscopy (SEM and TEM). Specific surface area was determined by the BET method using a sorptograph. The oxygen content was analysed by thermogravimetric method. Powder characteristics with respect to plasma conditions were analysed. The SiC powder generated was sintered in the presence of boron and carbide.

1. Introduction

During recent years, increasing attention has been given to the production of ultra-fine powders. This is based on the fact that metal or ceramic compacts made by sintering ultra-fine metallic or ceramic powders exhibit improved mechanical, physical and chemical properties. The ultra-fine powders of tantalum, molybdenum and tungsten were produced in a thermal plasma system in our laboratory [1]. In this work, our attention was focused on silicon carbides. It is well known that silicon carbide powder has promising applications in high-temperature technology [2], because of its unique properties such as high thermal shock resistance, good mechanical strength (high hardness and high resistance to wear, etc.), good chemical resistance (resistant to corrosion against acids and alkalines), especially its high thermal conductivity and low thermal expansion coefficient, and if SiC powder is ultrapure and ultra-fine, then its sintering characters can be improved.

In order to produce high-quality SiC powder the problem has been approached recently in different ways. Ishizaki *et al.* [3], Frederick *et al.* [4], Kong *et al.* [5], Nariki *et al.* [6] and Inoue *et al.* [7] produced ultra-fine β-SiC in d.c. plasma reactors. Kijima *et al.* [8], Cleaver *et al.* [9], Dow Corning Corporation [10], Kameyama *et al.* [11], Hollabaugh *et al.* [12] and Vogt *et al.* [13] generated ultra-fine β-SiC powder in r.f. plasma reactors. Kato *et al.* [14] and Okabe *et al.* [15] produce ultra-fine β-SiC in an SiC resistance furnace. Different starting materials were used by the above authors.

In the present work, the formation of SiC powders by the vapour phase reactions of $SiCl_4$–CH_4–H_2–Ar and CH_3SiCl_3–CH_4–H_2–Ar systems in a 15 kW d.c. plasma reactor was investigated. We attempted to produce ultra-fine SiC powder using industrial grade starting materials, $SiCl_4$, CH_3SiCl_3, H_2 and Ar, for further scale-up. The powder produced was characterized by X-ray diffraction and electron microscopy. The specific surface area was determined by the three-point BET method using a sorptograph (Quantasorb, Quantachrome Corporation). The oxygen content was analysed by thermogravimetry. The SiC powder was well sintered in the presence of boron and carbide.

2. Comparison of the different reactions

For production of ultra-fine SiC powder by vapour phase reactions, the following four reactions are usually used

$$SiH_4 + CH_4 \rightarrow SiC + 4H_2$$

reaction temperature 1300–1400 °C (1)

$$(CH_3)_4Si \rightarrow SiC + 3CH_4$$

reaction temperature 900–1400 °C (2)

$$CH_3SiCl_3 \rightarrow SiC + 3HCl$$

reaction temperature greater than 2000 °C (3)

$$SiCl_4 + CH_4 \rightarrow SiC + 4HCl$$

reaction temperature greater than 2000 °C (4)

The reactivity of the silicon source increases in the following sequence: $SiCl_4$, CH_3SiCl_3, SiH_4, $Si(CH_3)_4$. The equilibrium constants of the above reaction systems are presented in Fig. 1 [15]. From this figure we can see that the value of $\log K_p$ or the formation of β-SiC increases in the following order: $SiCl_4 + CH_4$, CH_3SiCl_3, $SiH_4 + CH_4$, $(CH_3)_4Si$.

Reactions 3 and 4 have low equilibrium constants at low temperature, the nucleation rate to produce silicon carbide will be low [17]. A fairly high temperature must be required, for example greater than 2000 °C, for the production of SiC powder. It is more difficult for the forward reactions of Reactions 3 and 4 to proceed than those of Reactions 1 and 2. It was found

* Author to whom all correspondence should be addressed.

0022–2461 © *1993 Chapman & Hall*

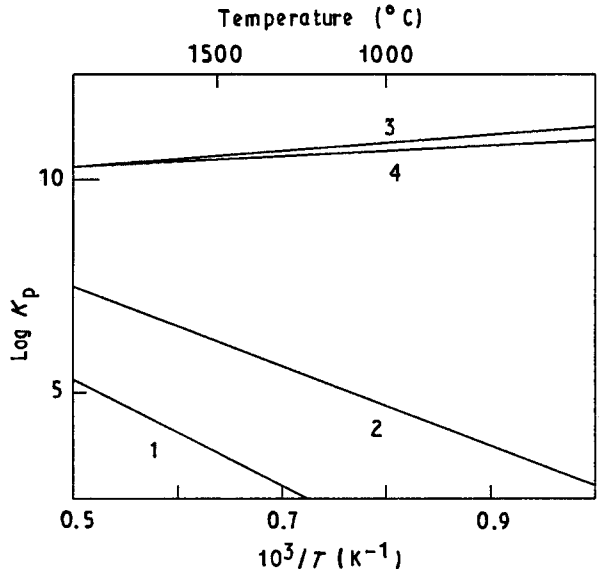

Figure 1 Equilibrium constants of β-SiC formation in several reaction systems: (1) $SiCl_4 + CH_4 \rightarrow SiC + 4HCl$; (2) $CH_3SiCl_3 \rightarrow SiC + 3HCl$; (3) $SiH_4 + CH_4 \rightarrow SiC + 4H_2$; (4) $(CH_3)_4Si \rightarrow SiC + 3CH_4$.

that systems of Reactions 3 and 4 can generate SiC powder just in the plasma condition.

The costs of the reactants decrease in following order: SiH_4, $(CH_3)_4Si$, CH_3SiCl_3, $SiCl_4$. In the present work, Reactions 3 and 4 have been studied to produce the SiC powder. The purity of the reactants used is listed in Table I.

TABLE I The purity of the reactants

Reactants	Grade	Purity	Company
Ar	High purity	99.996%	Linde
H_2	Extra dry	99.95%	Linde
N_2	Dry	99.7%	Linde
CH_4	Technical	97.0%	Linde
$SiCl_4$	Industrial	99%	Johnson & Matthey
CH_3SiCl_3	Industrial	98%	Johnson & Matthey

3. Experimental procedure

3.1. d.c. plasma CVD system

A block diagram of our d.c. plasma chemical vapour deposition (CVD) apparatus used is schematically drawn in Fig. 2; photograph is shown in Fig. 3.

The plasma gas is argon or a mixture of argon and hydrogen. The maximum values of the arc current and voltage are around 230 A and 59.4 V, respectively. The advantage of using the mixture of argon and hydrogen as plasma gas is that we can ensure a plasma gas with higher enthalpy (a pure hydrogen plasma can have an enthalpy of between about 11 000 and 33 000 kcal kg^{-1}), and a stable discharge and a reducing atmosphere can be formed.

In addition to silicon tetrachloride and the organic compounds, it is generally advisable to introduce hydrogen into the reaction zone. Hydrogen may, if desired, be introduced by passing through the d.c. torch (in this case, hydrogen will work as a plasma gas also) or by injecting it into the reactor from the down-

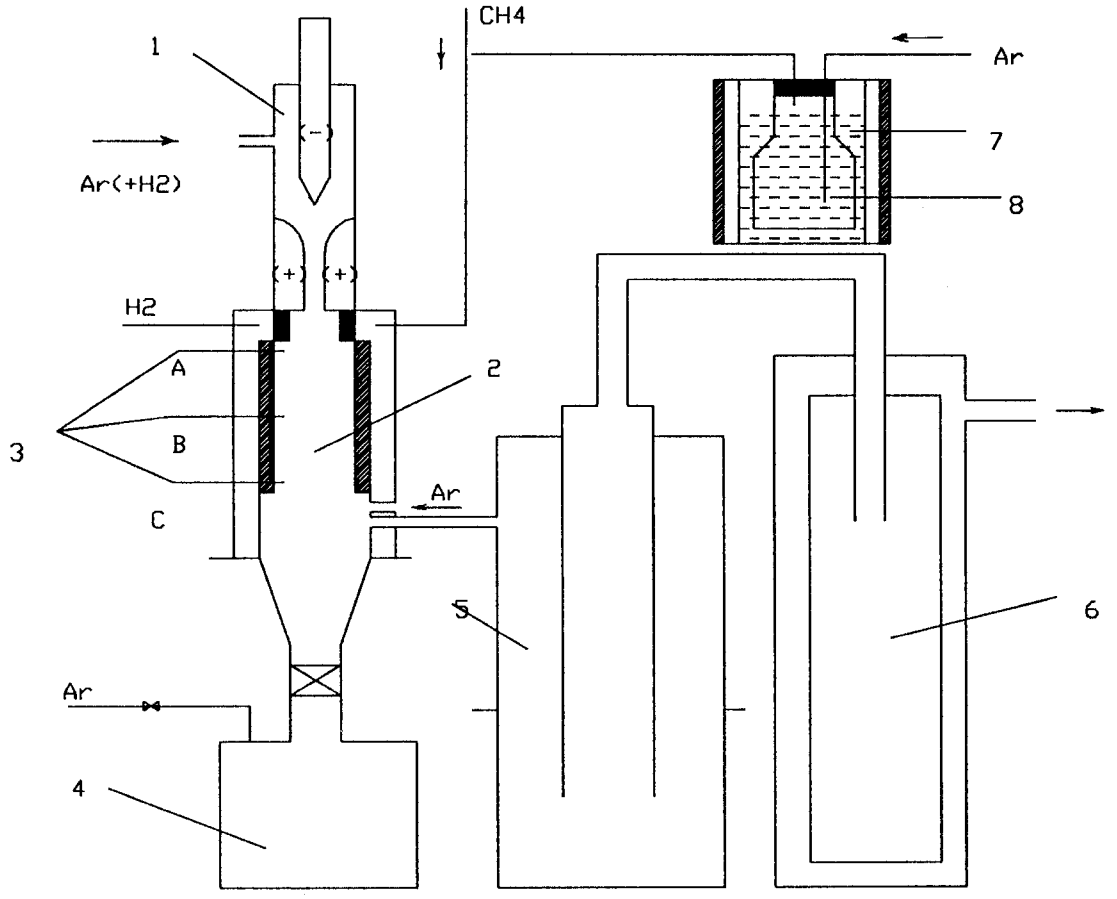

Figure 2 d.c. plasma system for the production of SiC powder. 1, Plasma torch; 2, reactor; 3, thermocouple; 4, collector; 5, cyclone separator; 6, bag filter; 7, feeding system; 8, evaporator.

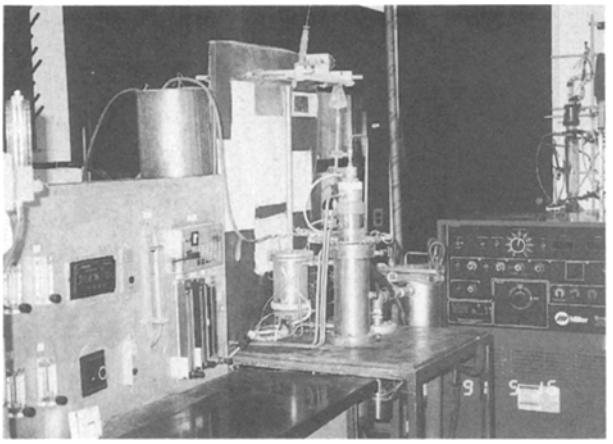

Figure 3 Photograph of d.c. plasma system for the production of SiC powder.

stream of the plasma, i.e. plasma tail flame. What is most important is that we must ensure the reactants reach the central hot zone, and also that the reactants are mixed uniformly. The reactants sprayed into the reactor should have a suitable velocity so that an appropriate resident time will be achieved. This can be done by adjusting the flow rate of the plasma gas, argon, or the argon amount in the plasma gas.

Four feeding ports (1.5 mm diameter) were kept radially just above the reaction chamber, equidistant from each other, to feed the gaseous or liquid reactants into the reaction chamber. The reactants can be kept separately or can be premixed before they are injected into the reactor, but the chemical reaction between reactants should be prevented outside the reactor, such as in the feeding tube as this would induce blockage of the feeding tube and feeding ports of the reactor due to the deposition of product. It is also necessary to heat the feeding tube of the reactants to an appropriate temperature. This will prevent condensation of the reactant vapour on the wall of the tube.

The reactants are placed in or are introduced into the feeding chamber and reaction chamber. The walls of these chambers should be resistant to the chemicals and should withstand high temperature. Graphite has been found to be very suitable for that purpose. The feeding chamber (25 mm inside diameter and 40 mm long) and the reaction chamber (50 mm inside diameter and 250 mm long), both made of high-quality graphite, are surrounded by a water jackets made with two concentric stainless steel tubes. Two observation windows are mounted radially opposite each other on the feeding chamber just below the torch exit, and are regarded as "O" section. Three thermocouple holes were provided. The first one located on the "A" section which is 62 mm from the "O" section. The second one located on the "B" section and the third one located on the "C" section which are 130 and 260 mm from the "A" section, respectively. The plasma characteristics and the situation of powder formation can be observed through the observation windows. Obviously the motion of the powder cloud near the observation windows can be seen when the reactions are taking place.

Our feeding system consists of an evaporator of the silicon source which is a glass bottle. It was kept in a water container at a constant temperature which could be adjusted to a desired value. The carrier gas, argon, passed through the bottle to carry the vapour from the silicon source into the feeding chamber. If the evaporator temperature, carrier gas flow rate and the pressure in the feeding chamber are fixed, the feeding rate of the silicon vapour source can be monitored.

The hot reaction mixture is cooled on exit from the reaction chamber. The method which we are using is to spray the inert gas, such as nitrogen or argon, as quenching gas into the reaction mixture in the quenching chamber. The gases with powder then passed through cyclone, bag filter and exhaust line, and finally went through a scrubber. To avoid contamination by adsorption, the temperature of the mixture gases should be above 100 °C on exit from the quenching chamber. This will assist in degassing of the product during collection.

A sampling collection device is connected to the bottom of the quenching chamber through a 4.0 cm valve. The powder sample can be kept in an inert protecting atmosphere to avoid oxygen contamination upon exposure to air.

Although the basic particle size is between 15 and 80 nm, it is much too small to be separated by a cyclone and bag filter separator. However, there is enough agglomeration for efficient separation and collection. We could see that a small part of powder escaped with the gases into the scrubber when the operation starts, then the escaping powder was lessened with the operation (we once passed the exhaust gas into a water tank; a very small amount of powder was observed to deposit into the water). This verified that most of the powder formed in the gas mixture (even though it is ultra-fine) could be collected by the combination of the cyclone and bag filter.

3.2. Powder preparation

Ultra-fine silicon carbide powder was made by injection of $SiCl_4$, CH_4 and H_2 or CH_3SiCl_3, CH_4 and H_2 into the reaction chamber, i.e. the tail flame of the plasma. Experimental conditions for the production of silicon carbide powder with Reactions 3 and 4 are summarized in Tables II and III, respectively. The typical temperatures in the different sections of the reactor are shown in Table IV.

It was shown from the experiments that the molar ratio of hydrogen and silicon sources must be greater than 2, because the hydrogen promotes the decomposition and reduction of $SiCl_4$ and CH_3SiCl_3 to produce more silicon nuclei. The silicon nuclei formed subsequently react with the carbon generated from the decomposition of CH_4 or CH_3SiCl_3 at high temperature and form SiC powder. The excess carbon in the SiC powder may be controlled by adjusting the amount of hydrogen and methane in the reaction gas mixture. An excess amount of pure hydrogen is always necessary in production of SiC powder.

The composition of the silicon carbide powder could vary over a wide range from excess silicon to

TABLE II Experimental conditions for the production of silicon carbide powders by Reaction 3

Run	Plasma gas, Ar ($ft^3 h^{-1}$)[a]	Plasma gas, H_2 ($ft^3 h^{-1}$)[a]	Power (kW)	CH_4/CH_3SiCl_3	Colour of powders
1	50	1.1	9.0	0.00	Yellow–grey
2	50	1.1	9.0	0.05	Grey
3	50	1.1	9.0	0.11	Dark grey
4	50	1.1	9.0	0.17	Light black
5	50	1.1	9.0	0.21	Black
6	50	1.1	9.0	0.32	Dark black
7	50	1.2	11	0.05	Black

[a] $1 ft^3 h^{-1} \simeq 2.8317 \times 10^{-2} m^3 h^{-1}$.

TABLE III Experimental conditions for the production of silicon carbide powders by Reaction 4

Run	Plasma gas, Ar ($ft^3 h^{-1}$)[a]	Plasma gas, H_2 ($ft^3 h^{-1}$)[a]	Power (kW)	$CH_4/SiCl_4$	Colour of powders
8	50	1.1	9.0	0.69	Yellow
9	50	1.1	9.0	0.93	Yellow–grey
10	50	1.1	9.0	1.08	Grey
11	50	1.1	9.0	1.15	Light black
12	50	1.1	9.0	1.39	Black
13	50	1.1	9.0	1.60	Dark black
14	50	1.2	11.0	1.15	Black

[a] $1 ft^3 h^{-1} \simeq 2.8317 \times 10^{-2} m^3 h^{-1}$.

TABLE IV Typical temperatures on the different sections of the reactor

Run	Temperature (°C)			
	O	A	B	C
2	> 2000	1600	1360	1200
10	> 2000	1550	1300	1150

excess carbon. The only change made here was the methane flow rate in Runs 1–6 in Table II. The colour of the powder clearly showed the difference. The β-SiC powder with excess silicon was yellow in colour; the β-SiC powder without excess silicon or carbon was grey in colour. The colour changed from grey to light black, black and to dark black as the excess carbon present in the SiC powder increased. Then in Runs 2 and 7, the plasma power was changed from 7 kW to 11 kW and the corresponding change of hydrogen content in the plasma gas (argon was kept constant as shown in the table) was from 1.1 $ft^3 h^{-1}$ to 1.2 $ft^3 h^{-1}$ ($\sim 3.114 \times 10^{-2} m^3 h^{-1}$ to $3.398 m^3 h^{-1}$), as shown in Table II. The colour of the β-SiC powder changed from grey to black. The possible reaction is that more carbon was generated by the decomposition of CH_4 in Run 7 than in Run 3. This is because in Run 7 higher plasma power afforded a higher temperature in the tail flame than in Run 3, and both the higher temperature and higher hydrogen atmosphere promoted the decomposition of CH_4. A similar situation occurred in Runs 10 and 14.

From our experiments, we observed some interesting phenomena. There was some solid deposition on the wall of the feeding chamber, especially near the feeding ports. However, this phenomenon appeared more often in the $SiCl_4 + CH_4$ system than in the $CH_3SiCl_3 + CH_4$ system. Another interesting phenomenon was that in some cases an SiC tube formed by crystal growth on the exit from the plasma torch. Its inside diameter is the same as the anode inside diameter. Its wall thickness and length could reach upto 2 and 20 mm, respectively. This could be eliminated by improving the inlet condition and reaction parameters. These phenomena will be discussed in another paper in detail.

3.3. Sintering of SiC powder

The SiC powder was sintered using additives of boron and carbon in the graphite furnace in an argon atmosphere. First, the SiC powder was mixed with amorphous boron and phenolic resin in the isopropyl alcohol in the appropriate composition. The mixture was dried at 60 °C. The dried slurry was pulverized by a mortar and the pulverized powder was filled into a stainless steel die. Then it was pressed at room temperature to a compact disc (green density > 60% theoretical density, TD) under a pressure between 15 000 and 25 000 psi.* Finally the disc was sintered in the graphite furnace at a peak temperature about 2100 °C for about 1–3 h in argon atmosphere. The heating time from room temperature to 2000 °C was about 4 h. The sample was allowed to cool to room temperature in the furnace.

* 10^3 p.s.i. = 6.89 $N mm^{-2}$.

4. Results and discussion

4.1. Characteristics of SiC powder

The typical X-ray diffraction patterns of β-SiC powder produced from Reactions 3 and 4 are shown in Figs 4 and 5, respectively. Typical transmission electron micrographs are shown in Figs 6 and 7, respectively, and typical electron diffraction patterns in Figs 8 and 9, respectively. The specific surface area was determined by the three point BET method using a sorptograph. The oxygen content in the SiC powder was measured by thermogravimetry. Table V shows the characteristics of the β-SiC powder.

Table VI shows the yield of SiC powder under different conditions. The yield was calculated from the total feeding rate of $SiCl_4$ and CH_3SiCl_3 and the weight of the collected powder. These figures are approximate values, because some powder escaped into the scrubber through the bag filter. The yield obtained for the system of Reaction 3 was slightly higher than that for Reaction 4, because the reactivity of CH_3SiCl_3 is larger than the reactivity of $SiCl_4$, as mentioned earlier.

In Figs 4 and 5, the major peaks of SiC powder appeared at around diffraction angles of 35.6°, 41.3°, 60.1°, 72.1° and 75.5°. These peaks are associated with a cubic crystal structure of β-SiC. Sometimes a peak appeared at around diffraction angles of 33.7° on Fig. 4. This peak is a characteristic of α-SiC with 4H and 15R structures. The higher temperatures favoured the production of high-temperature stable α-SiC. The peaks from the excess silicon produced can be seen on the X-ray patterns. When the silicon peaks did not appear on the X-ray patterns, it indicated that there was no excess or only a very small amount of excess silicon present in the SiC powder. Most of the excess carbon did not produce peaks on the X-ray patterns; presumably the excess carbon in the SiC powder is amorphous. Through high-temperature treatment in a protecting atmosphere, some excess carbon might transform to the crystalline form, so it could produce a carbon peak at a diffraction angle around 26.5°.

The particle diameter of the SiC powder can be estimated from the Scherrer equation, $D = 0.89\lambda/\beta\cos(\theta)$, where λ is the wavelength of the characteristic X-rays, θ is the Bragg angle, β is the calibrated width of the half-height of the diffraction peak. The particle diameters are 32 and 28 nm associated with Figs 4 and 5, respectively.

Figs 6 and 7 show that the particle diameter of the SiC powder is in the range 16–80 nm for Reaction 3, and 16–60 nm for Reaction 4. The average particle diameter is about 48 and 38 nm, respectively. The specific surface area of the SiC powder determined by the BET method is 42.102 $m^2 g^{-1}$ (Reaction 3) which corresponds to a particle diameter of 35 nm, and 45.819 $m^2 g^{-1}$ (Reaction 4) which corresponds to a particle diameter of 30 nm. The SiC powder particle diameters from TEM, X-ray and BET are basically identical. The particles of SiC powder were spherical and polygonal for Reactions 3 and 4. Some agglomeration occurred in the reaction. The chain-like agglomeration is a characteristic of particles in this size

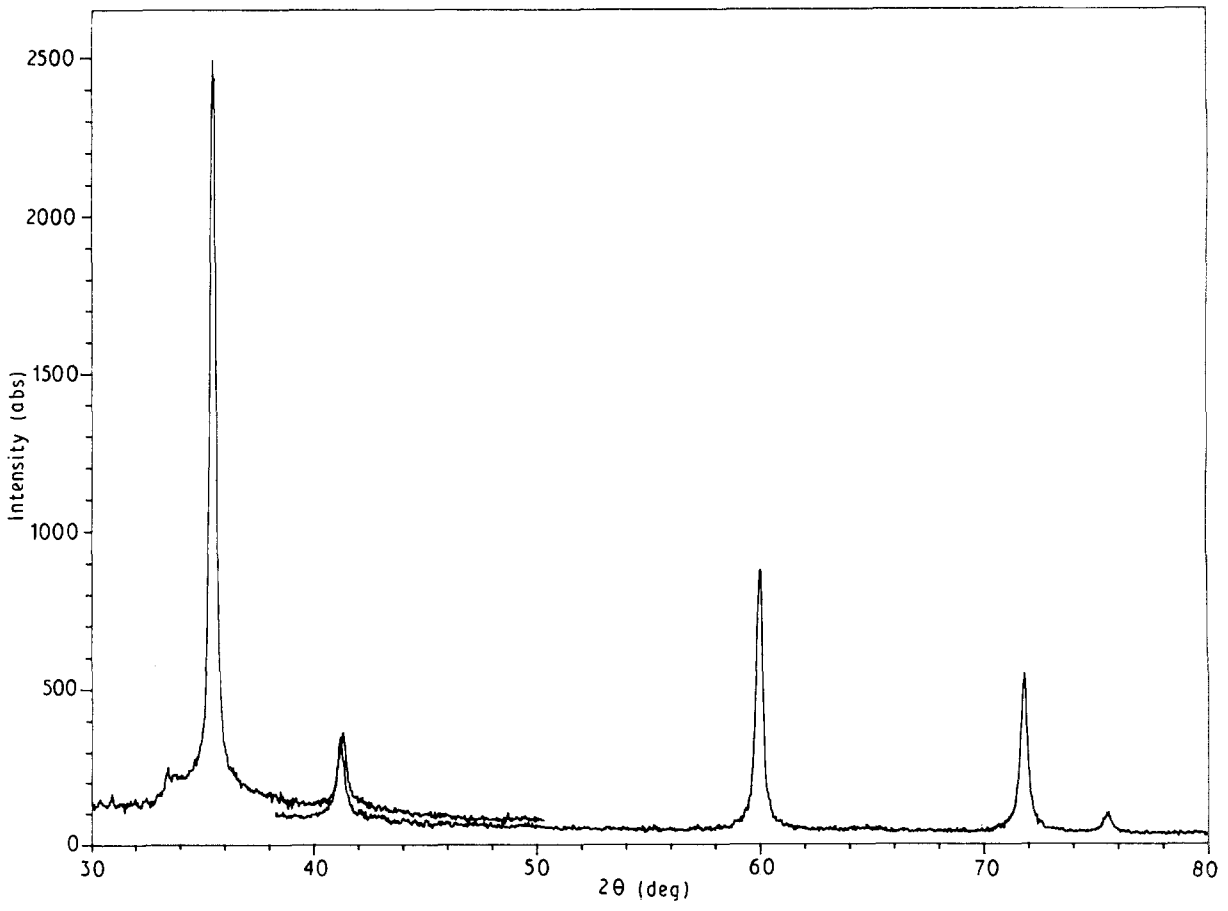

Figure 4 A typical X-ray diffraction pattern of the powder produced from Reaction 3 (Run 2).

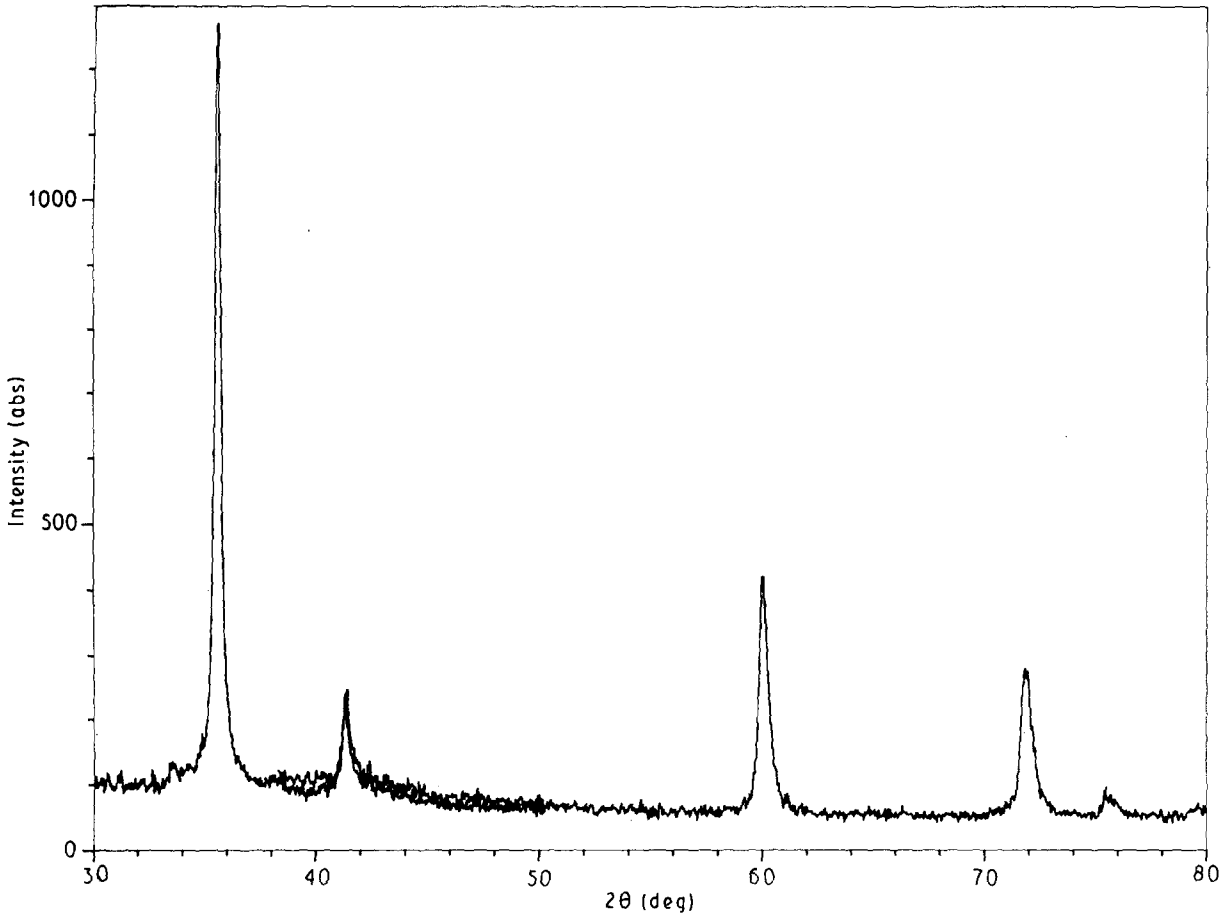

Figure 5 A typical X-ray diffraction pattern of the powder produced from Reaction 4 (Run 10).

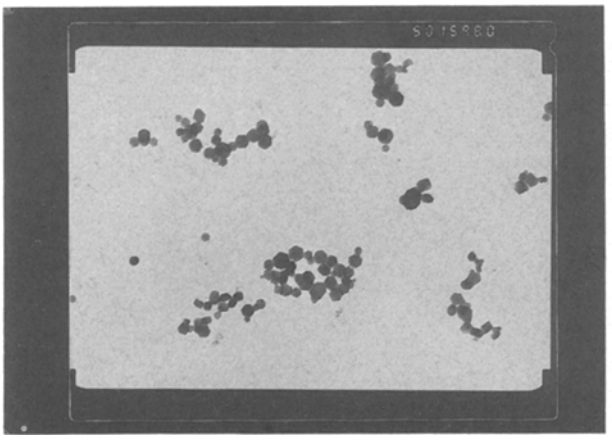

Figure 6 A typical transmission electron micrograph of the powder produced from Reaction 3 (Run 2). (Magnification 50 000).

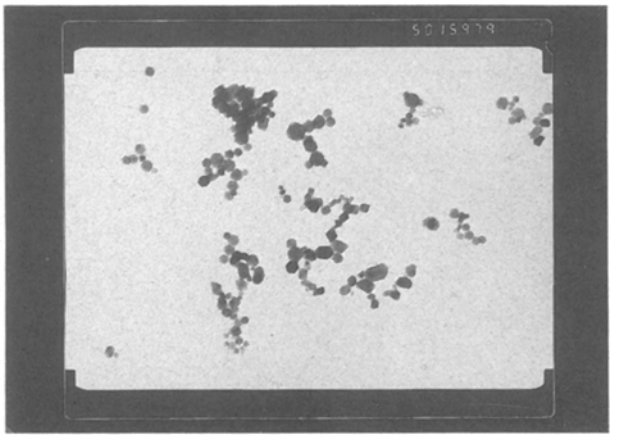

Figure 7 A typical transmission electron micrograph of the powder produced from Reaction 4 (Run 10). (Magnification 50 000).

TABLE V Characteristics of the β-SiC powders

	Reaction 3	Reaction 4	Sample in air	Sample in Ar
Particle diameter (nm):				
TEM	48	38		
BET	35	30		
X-ray	32	28		
Specific surface area $m^2 g^{-1}$ (BET)	42.012	45.806		
Oxygen content (%)			1.2	0.8
Excess silicon content: very small Excess carbon content: very small Sintering density: 86.0%–93.1% T.D.				

TABLE VI The yields of SiC powders

Run	Si source	Plasma gas Ar (standard $ft^3\ h^{-1}$)[a]	Total H_2 (standard $ft^3\ h^{-1}$)[a]	Power (kW)	Yield of SiC (%)
15	CH_3SiCl_3	50	4	9.0	81
16	CH_3SiCl_3	50	4	11.0	83
17	$SiCl_4$	50	4	9.0	80
18	$SiCl_4$	50	4	11.0	76

[a] $1\ ft^3\ h^{-1} \simeq 2.8317 \times 10^{-2}\ m^3\ h^{-1}$.

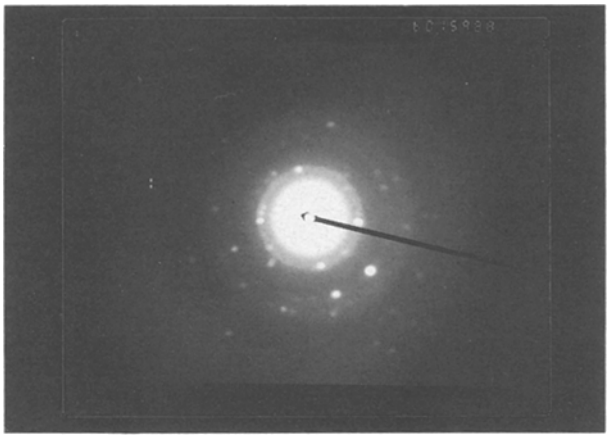

Figure 8 A typical electron diffraction pattern of powder produced from Reaction 3 (Run 2). (Magnification 140 000).

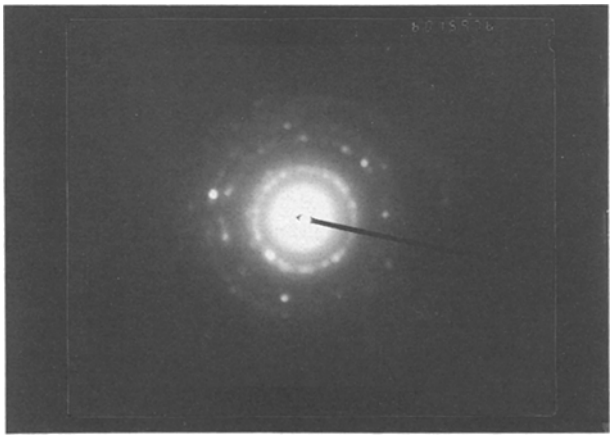

Figure 9 A typical electron diffraction pattern of powder produced from Reaction 4 (Run 10). (Magnification 100 000).

range. Figs 8 and 9 indicate that the particles are polycrystalline.

Some other obvious differences for the SiC powder produced by Reactions 3 and 4 were observed: smaller size and larger specific surface for the powder from Reaction 4; higher XRD intensity and the appearance of an α-SiC peak at $2\theta = 33.7$ for Reaction 3.

The oxygen content in the SiC powder sampled in air is about 1.2 wt % and when sampled in an argon atmosphere is less than 0.8 wt %. Ultra-fine powder is considered to be easily oxidized and adsorbs water on the surface in air. The Si–O bonding was analysed by infrared spectroscopy. It showed that the surface of the ultra-fine β-SiC powder was not covered with a thin film of oxidized silicon; the oxygen content was considered to be in the adsorbed water on the surface of the β-SiC powder [10].

TABLE VII Sintering results of SiC powders

Blend	Boron (%)	Carbon[a] (%)	TD[b] (%)	TD[c] (%)
1	0.15	2	80.7	86.0
2	0.20	3	89.0	89.5
3	0.25	2	93.1	92.3
4	0.30	3	90.0	91.0

[a] The carbon was in excess; we did not count the original excess carbon.
[b] For Reaction 3.
[c] For Reaction 4.

The amount of excess carbon in the SiC powder was usually controlled to about 1 wt %, but sometimes it was higher than 1%, for example 1–3 wt %. A small amount of excess carbon in the SiC powder is beneficial because it may act as a scavenger for oxygen or elemental silicon that may be present in the powder. It is possible to control the excess carbon content in SiC powder to between 1 and 3 wt % by plasma synthesis.

4.2. Sintering of SiC powder

The results of sintering are given in Table VII.

A typical X-ray diffraction pattern and a typical scanning electron micrograph of the fracture surface of a sintered body of SiC powder produced from Reactions 3 and 4 are shown in Figs 10–14, respectively.

As shown in Figs 10 and 12, some peaks of α-SiC appeared. It is assumed that some crystallization transfer from β-SiC to α-SiC took place in the sintering process. Figs 11 and 13 indicate that the microstructure of sintered SiC from the ultra-fine powder is fine and homogeneous. So it is hoped that the sintering density could be further increased. Both figures indicate that some carbon and pores are present. However, silicon, carbon and pores are present in Reaction 4, as shown in Fig. 14. Table VII shows that the sintering densities are between 86.0% and 93.1% TD. It is assumed that the density can still be increased if the sintering temperature is higher than 2100 °C. Some authors [16] have indicated that at a maximum temperature of approximately 2538 °C, silicon carbide can be sintered to 98% TD. Of course, the sintering density could decrease due to SiC evaporation when the sintering temperature is too high. The

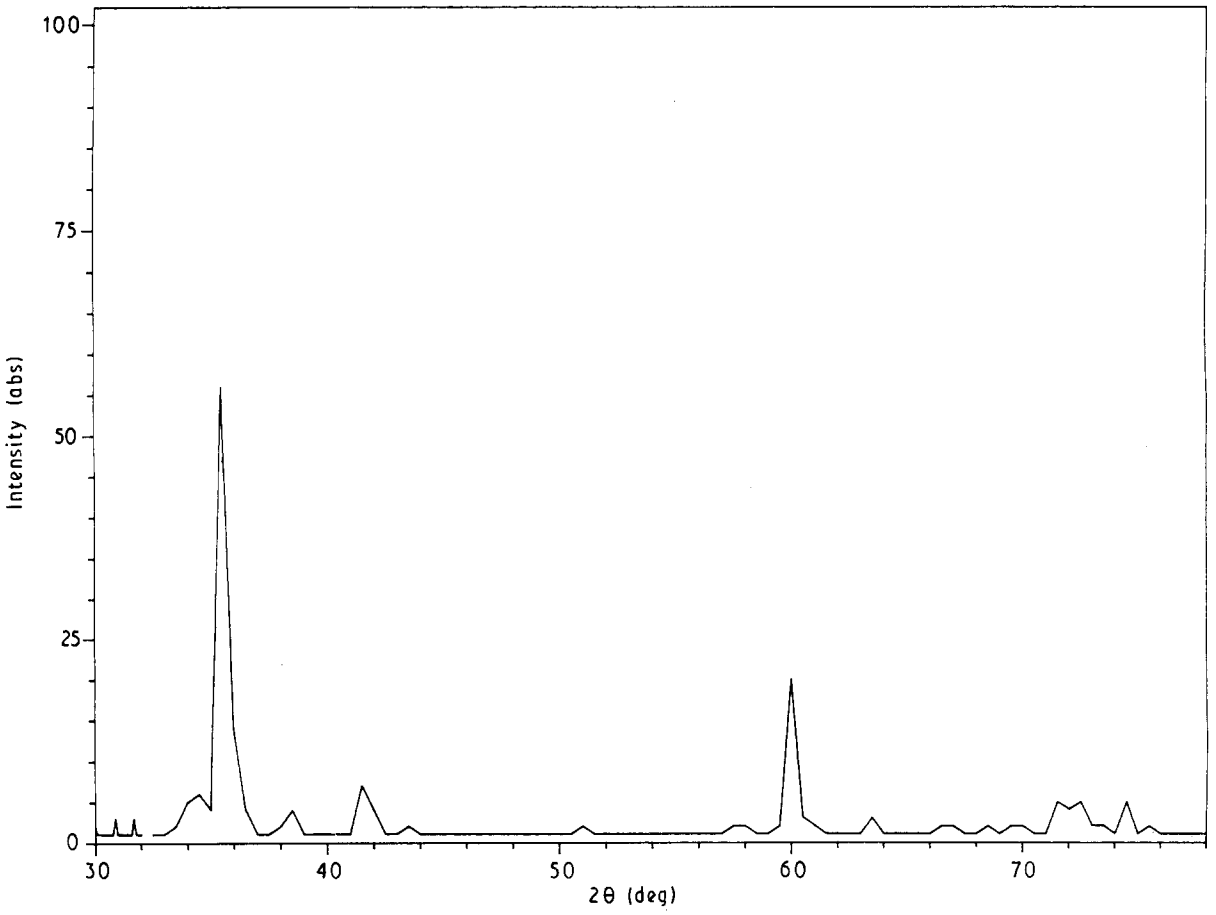

Figure 10 A typical X-ray diffraction pattern (Run 9) of a sintered body of SiC powder produced from Reaction 3 (Run 2).

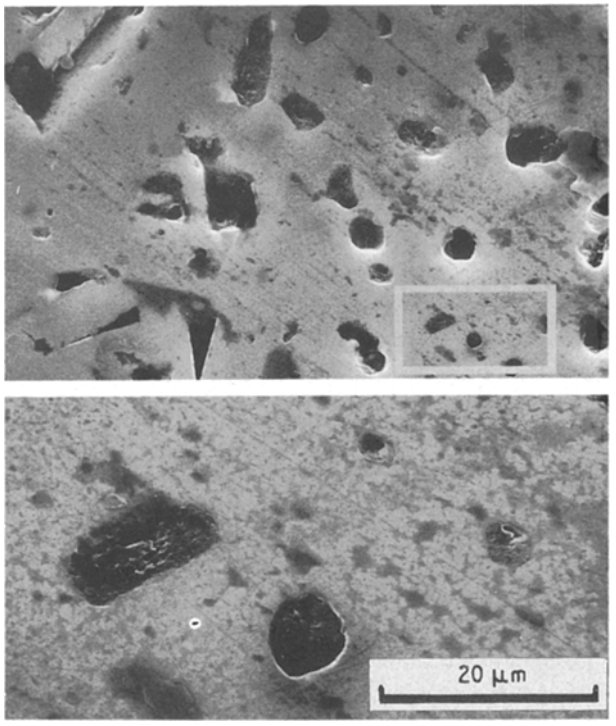

Figure 11 A typical scanning electron micrograph of fracture surface of sintered body of SiC powder produced from Reaction 3 (Run 2).

key problems for improving sintering density lie in (1) suitable sintering technology and parameters, e.g. sintering temperature, sintering time, press pressure of the sample, (2) suitable treatment of SiC powder before sintering, e.g. especially reducing the amount of oxygen, excess silicon and excess carbon, etc.

It is well known that oxygen and silicon contamination hinder densification of SiC powder. In particular, an oxide layer, e.g. a silicon oxide layer, around silicon carbide particles, forms a diffusion barrier which inhibits grain growth. The excess carbon can react with oxygen at the sintering temperature to produce carbon monoxide or carbon dioxide, thereby removing oxygen from the sintered parts. This means that a small amount of carbon present in the SiC powder could improve its sintering characteristics. However, large amounts of carbon in the SiC powder can appear to be undesirable inclusions in the microstructure.

From Table VII we can see that the sintering characteristics of both Reactions 3 and 4 are basically identical.

4.3. Control and treatment of contaminations

The control and treatment of the contamination level in the SiC powder is essential. The oxygen content in SiC powder can be decreased by (1) careful recovery, e.g. degassing techniques, (2) limiting the oxygen content of the starting materials, (3) prohibiting the leakage of the plasma CVD system. The elemental silicon content in the SiC powder can be controlled by monitoring the ratio of the source carbon and silicon reactants. The amount of carbon source reactant should be in at least stoichiometric quantities. We can see that the elemental silicon did not exist when the

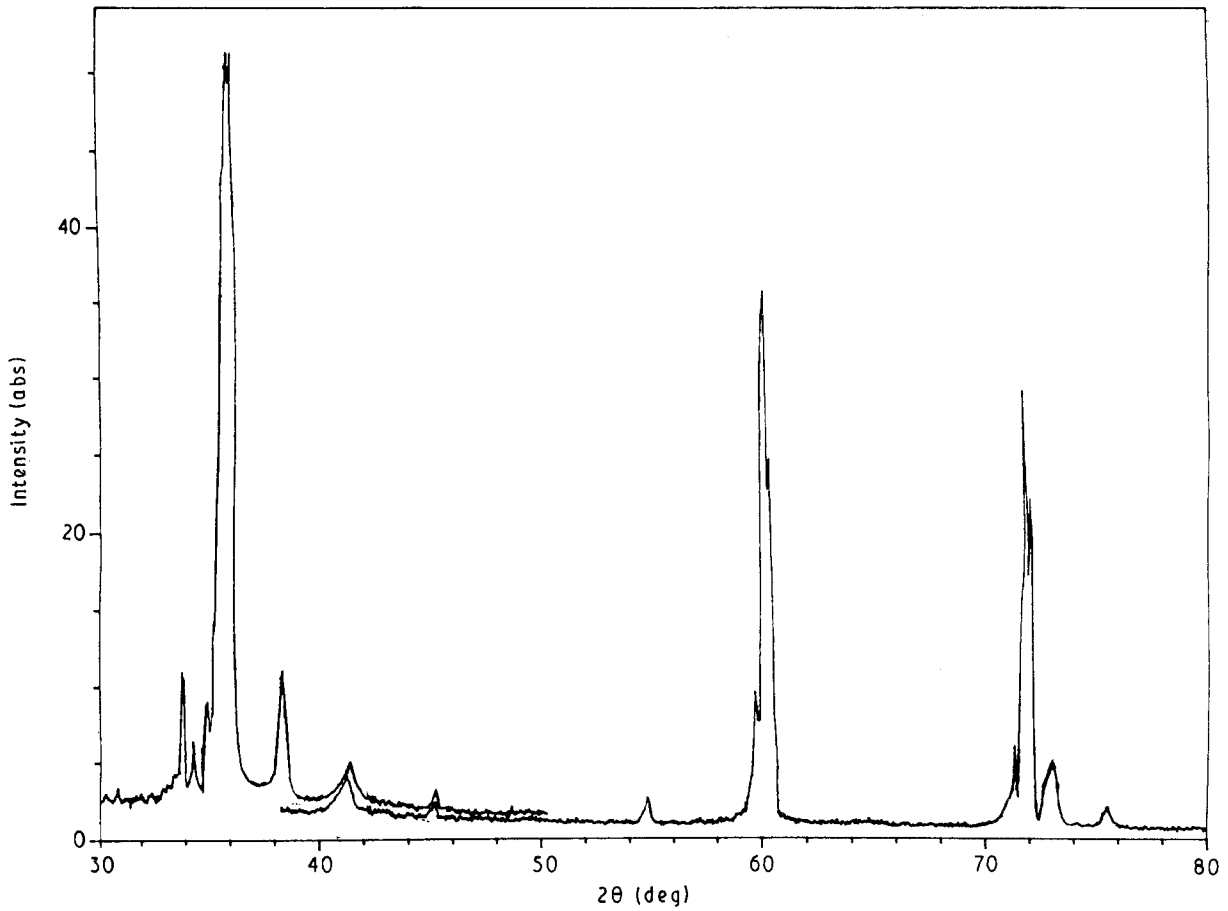

Figure 12 A typical X-ray diffraction pattern of a sintered body of SiC powder produced from Reaction 4 (Run 10).

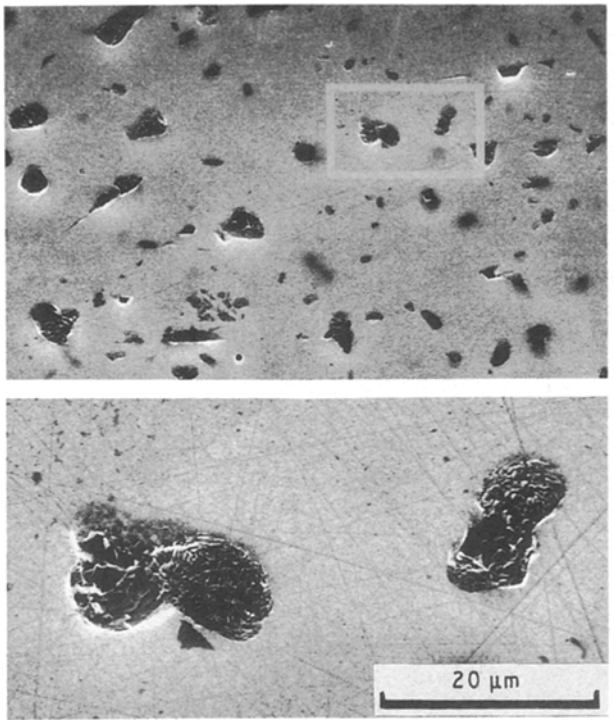

Figure 13 A typical scanning electron micrograph of the fracture surface of a sintered body of SiC powder produced from Reaction 3 (Run 10).

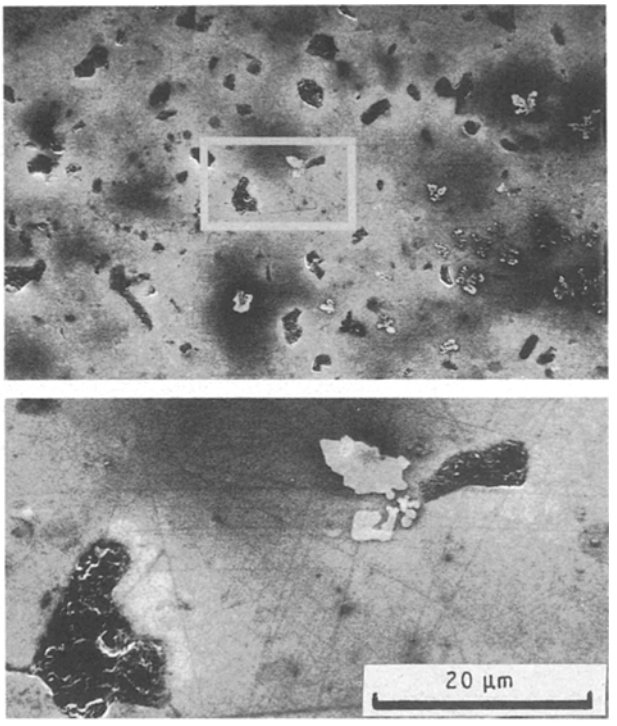

Figure 14 A typical scanning electron micrograph of the fracture surface of a sintered body of SiC powder produced from Reaction 4 (Run 9).

source ratio was about 1.1. The elemental silicon can be removed with hydrofluoric and nitric acids treatment even though a small amount of elemental silicon exists in the SiC powder [16]. The amount of excess carbon in the SiC powder is between 1 and 3 wt %. The excess carbon can be floated off in a water flotation cell [16], or eliminated by heating the mixed product in air at 800 °C [6, 9]. However, there was no

indication of a change in oxygen content in the SiC powder after the treatment.

The metal impurities, iron and copper, are the major contaminations for the production of ultra-fine metal powder in d.c. plasma [1]. Iron comes mainly from the corrosion of the feeding system of the reactants and the collection system of the powder. This can be decreased largely by improving the system materials and avoiding or decreasing corrosion. Copper comes mainly from evaporation of the copper anode in the plasma. It is estimated that the copper content in the SiC powder was about 70 p.p.m., based on our early experimental results [1]. Most of the other metal impurities were contained originally in the starting reactants. Metal impurities (analysed as elemental metal) represent less than 1000 p.p.m. of the silicon carbide powder, e.g. less than 0.1 wt %, and often represent less than 800 p.p.m. (0.08 wt %) [5]. To avoid contamination by adsorption, the powder collector can be heated to temperature above 100 °C to assist in degassing of the product during collection of the powder. In the event, the SiC powder product contains absorbed chlorine-containing species, e.g. halides of silicon, which can be removed by heating the product to about 600 °C, for about 2 h.

5. Conclusions

1. A d.c. plasma CVD system has been developed to produce the ultra-fine SiC powder. The characteristics of the powder can be controlled by the adjustment of the operating conditions of the plasma flame and the amount of reactants.

2. Using industrial grade materials $SiCl_4$, CH_3SiCl_3, CH_4, Ar and H_2, it is feasible to produce high-quality ultra-fine SiC powder. This is important progress enabling us to scale-up the plasma reactor for the industrial application.

3. A high sintering density may be expected by improving the sintering technology and sintering parameters for ultra-fine SiC powder produced from the plasma reactor.

4. The powder characteristics and the sintering characteristics for these powders generated from $SiCl_4$ and CH_3SiCl_3 are basically identical, but some differences were observed, i.e. smaller size and bigger specific surface for the powder from Reaction 4; higher intensity in X-ray diffraction and the appearance of α-SiC peak at $2\theta = 33.7°$ for powder from Reaction 3. However, the powder yields from Reaction 3 are slightly higher than from Reaction 4.

References

1. C. W. ZHU, G. Y. ZHAO, V. V. S. REVANKAR and V. HLAVACEK, *J. Mater. Sci.* **27** (1992) 2211.
2. C. W. ZHU, *Adv. Mech.* **16** (1986) 281.
3. K. ISHIZAKI, T. EGASHIRA, K. TANAKA and P. B. CELIS, *J. Mater. Sci.* **24** (1989) 3553.
4. FREDERICK G. STROKE and PA. McMURRAY, US Pat. 4295890, October 1981.
5. P. KONG, T. T. HUANG and E. PFENDER, *IEEE Trans. Plasma Sci.* **PS-14**(4) (1986) 357.
6. YASUFUMI NARIKI, YASUNOBU INOUE and KOHICHI TANAKA, *J. Mater. Sci.* **25** (1990) 3101.
7. YASUNOBU INOUE, YASUFUMI NARIKI and KOHICHI TANAKA, *ibid.* **24** (1989) 3189.
8. K. KIJIMA, N. NOGUCHI and M. KONISHI, *ibid.* **24** (1989) 2929.
9. DENIS CLEAVER, WILLIAM STANLEY WATSON and ARNOLD EVANS COULTHURST, UK Pat. Spec. 1 134 789 (1968).
10. Dow Corning Corporation, *Ind. Engng Chem. Prod. Res. Develop.* **11** (1972) 230.
11. T. KAMEYAMA, K. SAKANAKA, A. MOTOE, T. TSUNODA, T. NAKANAGA, N. I. WAKAYAMA, H. TAKEO and K. FUKUDA, *J. Mater. Sci.* **25** (1990) 1058.
12. C. M. HOLLABAUGH, D. E. HULL, L. R. NEWKIRK and J. J. PETROVIC, *ibid.* **18** (1983) 3190.
13. G. J. VOGT, R. S. VIGIL, L. R. NEWKIRK and M. TRKULA, Proceedings on the 7th International symposium on Plasma Chemistry, Eindhoven, The Netherlands, edited by C. J. Tummermans (1985) Vol. 2, pp. 668–673.
14. AKIO KATO, JUNICHI HOJO and TAKANOVI WATARI, in "Emergent process methods for high-technology ceramics", edited by Robert F. Davis, Hayne Palmour 3 and Richard L. Porter, Materials Science Research, Vol. 17 (Plenum Press, New York, London, 1984) pp. 123–135.
15. Y. OKABE, J. HOJO and A. KATO, *J. Less-Common Metals* **68** (1979) 29.
16. R. A. ALLIEGRO, L. B. COFFIN and J. R. TINILEPAUGH, *J. Amer. Ceram. Soc.* **39** (1956) 386.
17. YI CHANG and E. PFENDER, *Plasma Chem. Plasma Proc.* **7** (1987) 275.

Received 6 August 1991
and accepted 7 May 1992